Effects of environmental and operational variability on the spectrally selective properties of W/WAlN/WAlON/Al_2O_3–based solar absorber coating

A. Dan[a], B. Basu[a,b,*]

[a] *Materials Research Centre, Indian Institute of Science, Bangalore-560 012, India*
[b] *Interdisciplinary Centre for Energy Research, Indian Institute of Science, Bangalore-560 012, India*

T. Echániz, I. González de Arrieta and G.A. López
Applied Physics II, Faculty of Science and Technology
University of the Basque Country (UPV/EHU)
Barrio Sarriena s/n, 48940 Leioa, Spain

H. C. Barshilia[*]
Nanomaterials Research Laboratory, Surface Engineering Division, CSIR-National Aerospace Laboratories, HAL Airport Road, Kodihalli, Bangalore 560 017, India

[*]Corresponding Authors:
bikram@mrc.iisc.ernet (Bikramjit Basu), harish@nal.res.in (Harish C. Barshilia)

Abstract

The stability of solar selective absorber coatings in hostile environments (e.g., humid condition, corrosive medium, longer exposure at elevated temperature) needs to be critically assessed to ensure durability of such coatings. In the present work, magnetron sputtered W/WAlN/WAlON/Al_2O_3 –based absorber coating with a high absorptance and low emittance of 0.958 and 0.08 (82 °C) respectively, has been tested in humid and corrosive environments. The selectivity (absorptance/emittance) of the coating did not change after keeping it in a 95% humid environment at 37 °C for 400 hrs. Corrosion study in 3.5% NaCl solution reveals that this novel multilayer has a better corrosion resistance than that of uncoated stainless steel (SS) substrate. The nanoindentation test on the coating indicates that it has a hardness of 9.6 ± 0.5 GPa. The performance of the coating did not degrade after heat treatment at 350 °C in air for 1000 hrs. Additionally, the activation energy for degradation has been determined to predict the stability of the coating at high temperature. Further, the normal spectral emissivity of the tandem solar absorber was measured in the full angular range from 200 to 500 °C.

Emissivity measurements have been performed by varying observation angles. The results are analysed using numerical integration to obtain the total hemispherical emissivity. In summary, W/WAlN/WAlON/Al_2O_3 stack is an attractive candidate absorber coating which has potential to be used practically in photo-thermal conversion systems.

Keywords: Humidity, corrosion, activation energy, emissivity

1. Introduction

A spectrally selective solar absorber coating should possess a very high absorptance ($\alpha \geq 0.95$) in the solar spectrum (0.3 - 2.5 μm) and a low emittance ($\varepsilon \leq 0.05$) in the infrared region (2.5 – 25 μm) for an efficient photothermal conversion [1]. Along with the superior combination of absorptance and emittance, the absorber should also exhibit good performance at high temperature. Exceptional resistivity against thermal stresses, low thermal expansion coefficient, long thermal durability, thermo-chemical and thermo-mechanical stability are some of the critical parameters for solar selective absorber coatings [2]. These necessary properties can be assured by a multilayer structure where the metallic properties decrease from substrate to surface. During last few years, multilayer architectures, including TiAlSiN/TiAlSiON/SiO_2 [3], $Ti_{0.5}Al_{0.5}N/Ti_{0.25}Al_{0.75}N$/AlN [4], RuO_2/SiO_2 [5], HfMoN/HfON/Al_2O_3 [6], etc. have been studied extensively.

Long term durability of the absorber coatings can be determined by investigating their behaviours in harsh environment as the functionality of the solar absorber coating can be affected by various environmental issues. Therefore, several experiments on these coatings are extremely needed to find out their performance in adverse conditions. There are a few studies on the selective coatings concerning their mechanical stability, corrosion resistance, properties in the humid environment, scratch resistance, etc. For example, Gao et al. [7] demonstrated anti-corrosion property of TiC/Al_2O_3 based solar absorber. Ti/AlTiN/AlTiON/AlTiO –based spectrally selective coating, developed by Barshilia [2],

exhibited a superior combination of high spectral selectivity, improved adhesion, UV stability, corrosion resistance and high thermal stability. Amri et al. [8] have evaluated elastic modulus and hardness of cobalt-based metal oxide ($M_xCo_yO_z$ with M = Mn, Cu, Ni) thin solar absorber films and observed that such coatings exhibit appreciable mechanical stability.

Along with physical and mechanical stability, the emittance of the spectrally selective coating at elevated temperature is extremely important as high temperature emittance determines the rate of heat loss from the selective absorber surface. The infrared emittance is the metric to evaluate how well a surface radiates thermal energy in the infrared wavelength range as compared to a perfect black body operating at the same temperature. The total hemispherical emissivity (ε) is represented as,

$$\varepsilon = \frac{W}{W'} \tag{1}$$

where W and W' are the radiant emission from a real and perfect black body, respectively [9]. The emittance of a body can also be determined using Plank's radiation law,

$$N_\lambda = \frac{\varepsilon_\lambda C_1}{\lambda^5[\exp(C_2/\lambda T)-1]} \tag{2}$$

where λ is the wavelength, T is the absolute temperature, and C_1 and C_2 are the Planck constants.

Emissivity of a material is dependent on temperature, wavelength and surface condition. It can have a value between 0 (perfect reflector - mirror) and 1 (perfect emitter - black body). The total hemispherical emissivity at a particular wavelength can be obtained by

$$\varepsilon_H(T) = \frac{1}{\pi}\int_0^{\pi/2}\int_0^{2\pi} \varepsilon_T(\theta, T)\ \cos\theta \sin\theta\, d\theta\, d\emptyset \tag{3}$$

where $\varepsilon_T(\theta, T)$ is the total directional emissivity and ε_H is the total hemispherical emissivity at temperature T [10].

The photothermal application of the absorber demands a very low emittance, i.e., less amount of heat loss at high temperature as thermal radiation from a surface increases

proportionally by T^4. Recently, a little research attention has been devoted to acquire overall understanding of the radiative properties of these coatings. For example, Setién-Fernández et al. [11] first introduced a radiometric characterization of Mo - SiO_2 –based double cermet coating at the entire working temperature range (150 – 600 °C). The emissivity study by Echániz et al. [12] on Mo – Si_3N_4 –based spectrally selective coating from 250 to 600 °C for different number of heating cycles proved good performance for high temperature photo-thermal application. In a separate study, the high temperature emissive property of TiAlC/TiAlCN/TiAlSiCN/TiAlSiCO/TiAlSiO –based multilayer absorber coating have been determined by Jyothi et al.[13]. It has been found that the coating exhibit promising selective properties up to 500 °C. Therefore, it can be interpreted that in order to evaluate the performance of solar selective coating in actual field, a complete knowledge of environmental stability and high temperature emissivity is essential.

In our previous work, we have designed a coating of W/WAlN/WAlON/Al_2O_3 with graded metallic structure, which showed an excellent selectivity with a high absorptance of 0.958 and low emittance of 0.08. The thickness of the individual layer of W, WAlN, WAlON and Al_2O_3 is found to be ~ 125, 40, 40 and 62 nm, respectively. The layers were clearly distinguishable in terms of compositional variation [14, 15]. We also investigated long term thermal stability of the coating and found that the coatings were thermally stable at 350 and 500 °C for 550 and 150 hrs, respectively in air [16, 17]. In the present study, the optical properties of the coating have been examined in humid environment. In order to support humidity resistance of the coating, the contact angle of the coating with water has also been measured. The corrosion studies have been performed on bare and coated stainless steel substrates using electrochemical technique. The coating/substrate adhesion has been investigated by scratch test. Most importantly, we report here the long term thermal stability of the W/WAlN/WAlON/Al_2O_3 coating at 350 °C in air. The emissive properties of the

coating have been explored from 200 to 500 °C. In order to understand the underlying optical phenomena of the coating in the entire spectrum, we have investigated the dependence of emissivity with angle of observation and have evaluated the total hemispherical emissivity of the coating.

2. Experimental

The W/WAlN/WAlON/Al_2O_3 -based solar selective coating, shown in Fig. 1, has been deposited on stainless steel substrates by DC and RF magnetron sputtering using highly pure (> 99.9%) W, Al and Al_2O_3 targets. The SS substrate was mechanically polished using emery paper, followed by diamond nanoparticle suspension. The deposition chamber was evacuated to a base pressure of 8.0×10^{-4} Pa by means of a rotary and turbo molecular pumps. W, WAlN, WAlON and Al_2O_3 layers were deposited successively in Ar, Ar + N_2, Ar + N_2 + O_2 and Ar + O_2 environments. The depositions were carried out at a substrate temperature of 300 °C. A number of parameters, such as target power, reactive gas flow, and deposition time were tailored to achieve a maximum solar absorptance and low thermal emittance. The details of the deposition method can be found elsewhere [14]. The thickness of the coating was ~ 315 nm.

To carry out the humidity test, the samples were placed at nearly 95% humidity at 37 °C for 400 hrs. The reflectance spectra of the coating were collected before and after humidity test. The surface wettability of the coating was studied by measuring contact angles using sessile drop method with distilled water. The inspection was performed by contact angle goniometer (Dataphysics OCA 15EC) and a microscope that combine together charge-coupled device (CCD) camera and digital imaging techniques under ambient condition. A dosing volume of 5 μL was dispensed on the coating with a speed of 0.10 μL/sec. The contact

angle of the samples was measured at three places and the value reported herein is the average of three measurements.

The corrosion behaviour of substrate and coating was performed using a three-electrode electrochemical cell set-up in a 3.5% sodium chloride solution under free air condition at room temperature. In the electrochemical cell, a platinum plate of 1 cm^2 area and an Ag/AgCl, 3 M KCl electrode were fixed as counter and reference electrodes, respectively. The experiment procedure has been demonstrated in detail elsewhere [18].

Scratch adhesion test was performed using nano scratch tester (Bruker's Scratch Test System, USA). The coating was scratched by a Rockwell diamond indenter with the tip radius of 200 μm with a linearly increasing normal load from 1 to 4.5 N for 1 mm distance at a speed of 0.02 mm/s. The hardness of the absorber coating was estimated using Hysitron Triboindenter, Minneapolis, MN, USA, equipped with a three-sided pyramidal Berkovich diamond indenter. The equipment records the load, *P* and penetration depth, *h* of the indenter with resolutions of 1 nN and 0.2 nm, respectively. A peak load P_{max} of 1000 μN with loading and unloading rate of 200 μN/sec was used. The recorded data were analysed using the standard Oliver-Pharr method [19] to obtain the hardness, H of the multilayer film.

The absorptance and emittance of the selective absorber were measured using solar spectrum reflectometer and emissometer (M/S Devices and Services). An UV-Vis-NIR spectrophotometer (PerkinElmer, Lambda 950), equipped with an integrating sphere was utilised to evaluate the reflectance spectra of the coating at the incidence angle of 0°. In order to evaluate thermal stability, the coating was subjected to 350 °C for 1000 hrs inside a tube furnace. The multilayer coatings were kept in the temperature range of 300 – 500 °C for 2h for determining the activation energy of degradation.

The spectral emissivity measurements were carried out in the 2 - 25 µm range between 200 and 500 ºC using the high accuracy HAIRL radiometer. Two identical W/WAlN/WAlON/Al_2O_3 samples (Sample A and Sample B), fabricated in same deposition condition were required to verify the reproducibility of the emissive properties in air as well as in vacuum at 500 ºC. The measurement method and its precision analysis and other experimental details appear elsewhere [11]. In this case, spurious radiations from the sample surface reflections of the infrared window emission and of the detector itself were avoided to increase the measurement precision. The measurements were made first in vacuum of 10^{-3} mbar and then in air. The temperature of the samples was measured by welding two K-type thermocouples directly to the coating substrate, since no electrical contact could be made to the multilayer system.

In order to investigate the change in the phase assemblage between the heat treated and as deposited coating, X-Ray Diffractometer (Bruker, D8) with Cu - K_α (40 kV, 40 mA, λ = 0.15406 nm) radiation was used in the 2θ range of 10 – 60°. The as-deposited and annealed coating were characterized by Raman spectroscopy (WITec 300). X-ray photoelectron spectroscopy with non-monochromatic Al - K_α radiation (1486.8 eV) was employed to find the change in chemical composition and bonding structure of the heat treated coating. The binding energies reported here were calculated with reference to C 1s peak at 284.5 eV with a precision of 0.1 eV. The surface topography of the coatings was investigated by atomic force microscopy (Bruker) in contact mode with a silicon nitride tip of radius 50 nm in contact mode.

3. Results

3.1. Stability in humid and saline environment

The spectrally selective as-deposited coatings were placed in high humid environment (at 95% relative humidity and 37 °C) with exposure time up to 400 hrs. Fig. 2(a) represents

the reflectance spectra of the coating before and after humidity test. The overlapping of all of the reflectance spectra reveals that W/WAlN/WAlON/Al_2O_3 multilayer coating possesses excellent moisture resistance. In order to confirm the moisture resistance and the self – cleaning properties of the absorber coating, dynamic contact angle measurement was carried out. The contact angle of water droplet on the absorber surface (inset of Fig. 2(a)) is found to be 103°. Such hydrophobic nature of the coating is very effective to prevent the coating from damages in outdoor application against humidity.

A simple corrosion resistance test provides an idea of the durability of the novel W/WAlN/WAlON/Al_2O_3 coating in corrosive environment. Fig. 2(b) shows the potentiodynamic polarization curves of SS and W/WAlN/WAlON/Al_2O_3 coating, deposited on SS substrate. A decrease in i_{corr} of the coating compared to SS substrate and the shift of applied potential (V) in the positive direction confirm a decrease in the corrosion rate, which signifies the coated stainless steel to possess improved corrosion resistance. This result also suggests that the coating is chemically inert and durable in NaCl environment.

3.2. Mechanical stability

The scratch resistance is also a prime factor for providing a good performance of thin films, especially in the case of a multilayer coating as the scratch resistance indicates the adhesive strength of the coating. The scratch test was repeated three times at different locations of the specimen with the normal load from 1 to 4.5 N. Fig. 3(a) represents the optical micrograph of scratch on the absorber coating. The image of the scratched area has been captured by optical microscope. No evidence of delamination around the scratched region has been observed from the optical analysis. Fig. 3(b) represents the change in normal and the frictional forces vs time during the scratch test. The absence of critical load, i.e., the normal load for damage also confirms that the coating did not peel off.

Fig. 3(c) shows *P-h* (load vs. penetration depth) response of W/WAlN/WAlON/Al_2O_3 film on SS substrate. Nanoindentation studies have been repeated on 9 independent locations of the film. Similar observations have been obtained from all the data points. The obtained values from all the experiments were averaged to determine the mechanical properties of the thin film. The multilayer exhibits an average hardness (H) of 9.6 ± 0.5 GPa.

3.3. High temperature stability

3.3.1. Long term annealing and activation energy

One of the important problems limiting the use of solar selective absorber coatings is the long-term durability of these coatings at high temperature. Fig. 4(a) indicates a slight change in the reflectance spectra beyond 1300 nm after heating the sample at 350 °C for 80 hrs which may appear due to the initial thermal exposure, experienced by the coating. The reflectance spectra do not change if heated for longer duration which is evidenced from identical reflectance spectra of the samples annealed for 600 and 1000 hrs. Also, no variation in the absorptance values (α = 0.924) of the heat treated samples for 600 and 1000 hrs appeared. We have performed some preliminary analysis to assess the activation energy of degradation of the coating. The short-term thermal stability study on the coating indicates that the coating was stable up to 500 °C in air for 2 hrs with an absorptance of 0.934 and low emittance of 0.11 (Table 1). The drastic decrease in absorptance (α = 0.80 – 0.82) and increase in emittance (ε = 0.50) were recorded at 550 °C. In the present work, the Arrhenius equation was used to calculate the activation energy (E_a) i.e. the energy barrier for the degradation

$$\ln(\Delta\alpha) = \frac{E_a}{RT} + constant \qquad (4)$$

Where $\Delta\alpha$, R and T are change in absorptance, universal gas constant and temperature, respectively.

Fig. 4(b) plots the variation of ln($\Delta\alpha$) against the inverse of absolute temperature (1000/T). The activation energy has been calculated from the slope of the straight line and it comes out to be approximately 61 kJ/mol. Such activation energy is indicative of a higher energy barrier for degradation to occur. This analysis demonstrates that W/WAlN/WAlON/Al_2O_3 coating on stainless steel substrate may withstand a high temperature for long time.

3.3.2. High temperature emittance

In this work, the emissivity of the coating is determined in two distinct approaches, (a) the variation of emissivity with temperature and (b) the variation with incident angles. Fig. 5(a) provides a representation of the effect of temperature on emissivity. The temperature range of 200 to 500 °C has been considered as substantial temperature window for high temperature applications of the spectrally selective coatings. All the emissive spectra in different temperatures have been found to remain same without any sign of degradation. The reproducibility of the emittance measurements at 500 °C were checked by acquiring the emittance of two equivalent samples (Sample A and Sample B) deposited in the same experimental conditions. The corresponding emissivity spectra have been shown in Fig. 5(b), which indicate that the emissivity values are highly reproducible. We have also compared the normal emissivity of the SS substrate and that of W/WAlN/WAlON/Al_2O_3 coating at 500 °C. It can be observed that the emittance of the coating is lower than the substrate beyond 4 μm, whilst below 2 μm, it reaches a value more than double to that of SS at 2 μm. This result illustrates the improved emittance properties compared to the bare stainless steel substrate. It is also interesting to note that the emissivity of the coating decreases with increasing wavelength at shorter wavelengths and remains almost constant around 15 – 25 μm. Such emissivity behaviour of the coating is appropriate and essential for the absorber on receiver tube. The spectral response of Sample A, investigated at 500 °C in vacuum also retains the similar optical behaviour like other samples, examined in air. The normal emissivity spectra

of as-deposited and heat-treated coating at 500 °C for 12 hrs have been showed separately in the inset of Fig. 5(b). This allows better visualization of the temperature dependence on emissivity. A closer look at Fig. 5(b) reveals a slight increase in the emissivity values from 3 to 6 μm. Significant differences, observed around 2.93 and 4.25 μm, are due to radiation caused by H_2O (room humidity) and CO_2 molecules [20]. The above described experimental observations at elevated temperatures therefore assure the excellent performance of the coating for high temperature solar selective applications.

In order to demonstrate the structural and chemical changes, XRD data of as-deposited and annealed coating have been presented in Fig. 6(a). The formation of WO_3 can be observed after heat treating the sample at 500 °C for 12 hrs in air. For further structural elucidation, Raman spectroscopy of as-deposited and heat treated coating was carried out. Fig. 6(b) shows the comparative analysis of Raman peaks of the coatings. Two featureless broad bands can be observed in the Raman spectrum of as-deposited coating, while an intense Raman peak at 202 cm^{-1} was associated with bending of O-W bond in the pure WO_3 at heat treated coating. To study the chemical composition and chemical state of various elements of the as-deposited and annealed absorber, the coatings were characterized by XPS. Fig. 7(a) shows the survey scan spectra of both the coatings. Appearance of a small W peak in the heat treated coating indicated the outward diffusion of W as expected. The XPS data were further analysed by recording the core-level spectra of two coatings. Typical Al 2p, O 1s and W 4f core level spectra of as-deposited and annealed coating have been presented in Fig. 7(b - d). Al 2p spectra of both the coatings represent the presence of Al - O bond with bonding energies at around 74.5 eV [21]. No significant change in Al 2p core level spectrum has been observed after annealing the coating in air. The O 1s spectrum of as-deposited coating shows a characteristic peak at a binding energy of 531.5 eV corresponding to the O 1s electrons in Al_2O_3 [22]. The O 1s spectrum of annealed coating has been deconvoluated into three distinct

components at 530.5, 531.5 and 532.9 eV [23, 24]. The peak at 531.5 eV originates from O 1s electron in Al_2O_3 as found in O 1s spectrum of the as-deposited coating. The peak centred at 530.5 eV, can be assigned to O 1s electrons in WO_3 [34]. The peak, centred at 532.9 eV, indicates the presence of WO_x [24]. The deconvolution of W 4f spectrum of heat treated coating resulted in two peaks, centred at 35.8 and 37.8 eV. These peaks originate from W $4f_{5/2}$ and W $4f_{7/2}$ electrons in WO_3 [25]. The appearance of these peaks is due to the formation of new WO_3 phase as a result of outward diffusion of W to the top layer. The XPS spectra thus confirmed the formation of WO_3 in the annealed coating.

The coating surface roughness is one factor that affects the selective properties of the coating by increasing the emittance. According to the general theory of scattering, the rougher the surface is, higher will be the emittance [26]. The surface topographies of the as-deposited and heat treated coatings were studied using AFM. The 3-dimensional AFM images of these coatings are shown in Fig. 8. The root mean square roughness values of the as-deposited and the heat-treated coatings are 2.6 and 3.1 nm, respectively. Hence it can be stated that W/WAlN/WAlON/Al_2O_3 coating retained the smooth surface morphology even after heat treatment at 500 °C for 12 hrs in air which helps the coating to exhibit the similar spectral emissivity property after annealing.

The emissivity of a sample is strongly dependent on the observation angles and this aspect is poorly studied for absorber coating. In the present study, we have analysed how emissivity varies when the observation angle increases. The directional emissivity values at different viewing angles from 10° to 80° for the wavelength range of 0 – 25 μm have been presented in Fig. 9(a). The emissivity of the coating decreases with an increase in viewing angle up to ~ 4.5 μm, shown in the inset of Fig. 9(a). Above this wavelength, a reverse phenomenon can be observed, i.e., the emissivity increases with increasing the angles. It can also be observed that upto 10 - 40°, only small variations in emittance have been observed.

At angles higher than 40°, the emittance increases considerably with detection angle. In addition, the results indicate that one maximum appears around ~ 10.6 μm and this increases as the observation angle increases. The peak appears due to the Berreman effect [27], which usually indicates the longitudinal (LO) phonon modes of Al – O bonds of Al_2O_3 [28]. For further clarification, the directional spectral emissivity has been represented as a function of viewing angle for several discrete wavelengths in Fig. 9(b). A gradual decreasing trend of emittance up to $\theta < 70°$ with the increase in viewing angle, followed by a sharp drop beyond $\theta \sim 70°$ have been observed for 2 and 3 μm wavelengths. For rest of the wavelengths (5, 10 and 15 μm), emittance increases slowly up to $\theta < 40°$ and reaches a maximum around 75°. For both the cases, the emittance drops to zero at 90°. As the multilayer is highly absorbing in solar and NIR spectrum, it causes higher values of emittance. Beyond that wavelength (~ 3 μm), the entire stack reflects most of the incident infrared wavelength to minimize the emittance.

Numerical integration of the directional spectral data as a function of temperature for both Sample A and Sample B, shown in Fig. 9(c), gives values of the total hemispherical emissivity. Such calculation shows significant improvement over previous studies wherein only the total normal emissivity was calculated. The same integration procedure was followed for the calculation of the total emissivity at each angle and they were integrated, according to Eqn. 3. The total hemispherical emissivity can be expressed by the following Eqn..:

$$\varepsilon_H(T) = a + 10^{-5}bT + 10^{-8}cT^2 + 10^{-10}dT^3 + \cdots \quad (5)$$

where T is the temperature and a, b, c, d are fitted coefficients. The total hemispherical emissivity values of both coatings were fitted to a polynomial of order 2 in order to obtain a phenomenological expression useful for heat transfer calculations when using these coatings in engineering applications (with T in °C):

$$\varepsilon_H(T) = 0.138 + 8.25 \times 10^{-6}T + 3.23 \times 10^{-7}T^2 \quad \text{(Sample A)} \quad (6)$$

$$\varepsilon_H(T) = 0.129 + 5.91 \times 10^{-6}T + 2.27 \times 10^{-7}T^2 \quad \text{(Sample B)} \quad (7)$$

The fitting as shown in Fig. 9(c) allows an interesting analysis of this type of selective coating as it can be clearly observed that there is a strong dependence of temperature on the total hemispherical emissivity, which increases with an increase in temperature. This investigation enables us to acquire an overall understanding of the actual behaviour of spectrally selective absorber coating at different operation temperatures for CSP applications.

4. Discussion

In this section, we will demonstrate the underlying reasons behind excellent mechanical, environmental and thermal stability of W/WAlN/WAlON/Al_2O_3 –based multilayer absorber coatings. At first, we will discuss about the moisture resistance and hydrophobicity of the absorber stack. These are essentially correlated with surface chemistry, which is determined by the characteristics of materials used. Pristine Al_2O_3 is hydrophilic in nature as it consists of a large number of polar sites originating from unsaturated aluminium and oxygen atoms. A hydrophilic structure is usually formed near surface to configure a full octate of electrons in electron-deficient aluminium atoms. It is interesting to note that the chemical or geometrical modification of a material can also govern the water repellence. Our results clearly indicate that in spite of the presence of Al_2O_3 on top layer, W/WAlN/WAlON/Al_2O_3 coating surprisingly possess hydrophobicity. It is quite likely that RF sputtering would lead to the deposition of nanocrystalline Al_2O_3 [14]. Although W/WAlN/WAlON/Al_2O_3 coatings have less surface roughness, it can be believed that hydrophobicity in the present case is intrinsic to the nanocrystalline nature of the magnetron sputtered coatings. This finding is also consistent with other coatings with similar surface roughness [29, 30]. Moreover, the ambient atmospheric exposure of magnetron sputtered

Al_2O_3 may result incorporation of hydroxyl to the oxide surface which may reduce the wettability of the thin film [31-33].

The result of humidity test (see Fig. 2(a)) revealed the high moisture resistance of the coating. High atmospheric humidity enhances condensation of moisture in the form of droplets which may lead to pin-holing, cratering and cracking. Additionally, condensation also causes blistering, blooming and eventually results to delamination of the coating. As the absorptance and emittance have not changed after exposure of the coating into humid environment, it can be stated that Al_2O_3 layer on top acted as a protective layer to tackle such detrimental phenomena.

Our results also unveil that W/WAlN/WAlON/Al_2O_3 –based coating not only has a superior water repellence property but also has significant resistance in corrosion environment. The corrosion can take place through the defects on the coating surface, such as micro cracks, pores, cavities, etc. The reasons behind the enhanced corrosion resistance of the present absorber coating can be attributed to the fact that the coating surface was very smooth and crack free. The composition of the coating has also played an important role towards corrosion resistance. The layer of Al_2O_3 on the top passivates the surface and acts as a barrier between the surrounding environment and the underlying coating. The corrosion behaviour of the multilayer coating has also been improved by the presence of Al in WAlN and WAlON layer as Alanyali et al. [34] reported that the incorporation of Al to the transition metal nitrides improves the corrosion resistance. It has also been reported that the coatings with high W content have an excellent corrosion resistance property [35]. In addition, stainless steel has a wide spectrum of resistance to corrosion by chemical environments [36].

The better mechanical stability of the coating was confirmed by the scratch test. It has been found that there was no detachment of the coating along the edges of the scratch test track. It is worthwhile to mention that the exceptional scratch resistance of the coating

appears due to nanocrystalline nature of WAlN, WAlON and amorphous nature of Al_2O_3 layer. The WAlN and WAlON layers are composed of nanocrystalline phase of AlN and WO_3, respectively and Al_2O_3 layer was amorphous in nature [14]. The scratch resistance can also be well correlated with the better resistance to plastic deformation of the coating. The plastic deformation of the nanocrystalline films [37] usually be prevented as these films (i) hinder the generation of dislocations, (ii) prevent crack propagation, and (iii) suppresses grain boundary sliding [38]. Moreover, the adhesion of the multilayer coating strongly depends on the initial layer, deposited on the substrate. As highly adhesive W has been deposited on SS substrate as interlayer, a good adhesion of the coating has been obtained. Additionally, WAlN layer improves the load bearing capacity and prevent fracture of the coating, which results in better adhesion [39].

In addition to improved environmental and mechanical properties, the high temperature emissivity of the coating should also be taken into account when these coatings are heat treated at 350 °C for 1000 hrs. The coating does not show significant changes in the spectral properties in solar spectrum regime (300 – 2500 nm) while heat treated for a prolonged duration. Not only that, it is clear from the emissivity measurements that emissivity spectra do not exhibit any drastic change after the heat treatment of the coating at 200 – 500 °C. It is well known that thermal radiative emissions from a material arise due to band-to-band transition, lattice vibrations and thermal motion of charges [40]. In Fig. 5(a), the emissive behaviour of the coating in solar spectrum (> 2.5 μm) is dominated by W/WAlN/WAlON/Al_2O_3 stack due to it's opaque nature in shorter wavelength while the emissive response at the rest of the spectrum is governed by W layer having inherently low emissivity values owing to the poor efficiency of photon emission from the surface. In the solar spectrum (0.25 - 2.5 μm), the emittance is fairly high. According to Kirchoff's law, emittance of a material represents the absorptance ($\varepsilon(\lambda) = \alpha(\lambda)$) at a particular wavelength.

Hence, the high emittance of the coating in > 2.5 μm suggests that most of the solar radiation is absorbed by the multilayer absorber, while the spectral emissivity in the infrared region (2.5 – 25 μm) is significantly less than in the region with shorter wavelength. The emissivity enhancement is essentially a consequence of the inter-reflections within the structure, which reduces the reflectivity and as a result, the emissivity and absorptivity are enhanced. The combination of nitride/oxynitride/oxide layers leads to destructive interference, causing lower values of emissivity in shorter wavelength range, while these materials may not have any influence on emissivity in longer wavelength and for that reason, emittance value above 5 μm remains constant. Different spectral response in these two separate wavelength regimes is desired for an efficient spectrally selective coating. The working temperature has also an effect on the emissivity of the material. Therefore, it is expected that the emissive properties of the coating will be influenced by annealing the samples in high temperature. After heating the sample at 500 °C for 12 hrs, no drastic difference in the spectral response in the heat treated coating has been observed. According to Brodu et al. [41] the emittance of W coating can remain stable up to very high temperature due to less sensitivity towards surface diffusion. Hence, it is expected that the presence of W interlayer on SS substrate assist to retain the similar emissivity characteristics at elevated temperature. From XRD, XPS and Raman study, it has been noticed that WO_3 forms after annealing the sample in air. The combination of Al_2O_3 and WO_3 on top layer play an important role as oxygen diffusion barrier and act as effective passivation layer between underneath layers and the environment. The selected layers namely, WAlN, WAlON and Al_2O_3 are highly stable in extreme conditions and these layers restrict interdiffusion between layers, structural transformations and chemical reactions.

Along with high temperature emittance, the angular dependence of emissivity was also investigated. The observable fact is that for lower wavelengths, the value of emissivity

decreases as the look angle increases. An increase in emissivity with increasing viewing angle does exist for longer wavelengths. For 2 and 3 μm wavelengths, emittance decreased slowly up to $\theta < 70°$ after which it dropped sharply, like a typical dielectric. On the other hand, the angular variation of emissivity at higher wavelengths (5, 10 and 15 μm) is dominated by W metal. These angular characteristics are not only related to the optical properties of the materials, but also related to various factors, like scattering mechanism, porosity, surface roughness, etc. [42-45].

The fitting of hemispherical emissivity values as a function of temperature (see Fig. 9(c)) may not only allow one to evaluate the thermal energy losses from a collector but also to understand the microscopic origin of the temperature dependence of the radiative properties of the coating. The increase in total hemispherical emittance as a function of temperature may be a direct consequence of phonon – phonon interactions and the enhancement of the population of phonons with the increase of the temperature [46].

It is worth mentioning that multilayer absorber based on WAlN and WAlON together with a W back reflection layer and anti-reflecting Al_2O_3 layer have formed a very effective selective absorber. This multilayer stack exhibits excellent spectral selectivity and high temperature stability simultaneously. The high temperature performance of the material can be corelated with the intrinsic material properties, structural integrity and adhesive nature of the coating with substrate. In the multilayer, W layer not only serves the role of infrared reflector to reduce the emissivity, but also acts as diffusion barrier and adhesion promoter on stainless steel substrate to hinder the diffusion of Fe and Cr atoms into rest of the layers. WAlN has been chosen as the main absorber layer as it is known to be thermally resistant to oxidation [47, 48].

Moreover, the combination of transition metal nitride and oxynitride has been widely used in solar selective coating for excellent thermal shock resistance as they are capable to

withstand sudden variation in temperature caused by clouds, thundershower, etc. [49-53]. Furthermore, Al_2O_3 has been introduced as anti-reflection layer to enhance the solar absorption remarkably as well as to protect the underneath layers from environmental degradation.

To summarize, W/WAlN/WAlON/Al_2O_3–based coating with excellent optical properties, outstanding environmental stability, mechanical robustness and long term durability at high temperature qualifies most of the criteria to be utilized as a spectrally selective absorber on receiver tubes of CSP systems.

5. Conclusions

W/WAlN/WAlON/Al_2O_3 –based coating with a high spectral selectivity ($\alpha = 0.958$, $\varepsilon = 0.08$) possess good environmental stability in highly humid and corrosive environment. The judicious selection of coating compositions allows the coating to exhibit a reasonably good scratch protection and considerably high hardness. Beyond mechanical and environmental stability, the coating also showed superior resistance against thermal degradation at 350 °C for 1000 hrs in air. The activation energy for degradation is found to be 61.4 kJ/mol. The presence of W and Al_2O_3 as inter-diffusion and antireflection layer protect the coating at high temperature and facilitate to retain the emissive property at 500 °C in air and vacuum for 12 hrs. The analysed angular variation of emissivity commensurate well with the spectrally selective nature of the multilayer stack. Overall, the combination of aforementioned optical, mechanical and thermal properties ensures the capability of the coating as an attractive absorber photo-thermal conversion systems with a promising durability.

Acknowledgments

This paper is based upon work supported in part under the USIndia Partnership to Advance Clean Energy-Research (PACE-R) for the Solar Energy Research Institute for India and the United States (SERIIUS), funded jointly by the U.S. Department of Energy (Office of

Science, Office of Basic Energy Sciences, and Energy Efficiency and Renewable Energy, Solar Energy Technology Program, under Subcontract DE-AC36-08GO28308 to the National Renewable Energy Laboratory, Golden, Colorado) and the Government of India, through the Department of Science and Technology under Subcontract IUSSTF/JCERDC-SERIIUS/2012 dated 22nd Nov. 2012. This research was partially supported by the research program of UPV/EHU. The authors acknowledge Mrs. Latha, Mr. Srinivas, Mr. Praveen, NAL for XPS, UV-Vis-NIR, XRD, AFM measurements. A special note of thanks is due to Mrs. Ezhil Selvi, NAL for her support in performing corrosion test. One of the authors, AD is grateful to Sharmistha Naskar, BSSE, IISc, Subrata Senapati, MRC, IISC, and Abhishek Chaturvedi, Materials Engineering, IISc for helping in humidity test, Raman spectroscopy measurements, and hardness test, respectively. AD thanks DST for providing INSPIRE scholarship during the period of study.

References

[1] A. Dan, H.C. Barshilia, K. Chattopadhyay, B. Basu, Solar energy absorption mediated by surface plasma polaritons in spectrally selective dielectric-metal-dielectric coatings: A critical review, Renewable and Sustainable Energy Reviews, 79 (2017) 1050-1077.

[2] H.C. Barshilia, Growth, characterization and performance evaluation of Ti/AlTiN/AlTiON/AlTiO high temperature spectrally selective coatings for solar thermal power applications, Solar energy materials and solar cells, 130 (2014) 322-330.

[3] L. Rebouta, P. Capela, M. Andritschky, A. Matilainen, P. Santilli, K. Pischow, E. Alves, Characterization of TiAlSiN/TiAlSiON/SiO_2 optical stack designed by modelling calculations for solar selective applications, Solar energy materials and solar cells, 105 (2012) 202-207.

[4] M. Du, X. Liu, L. Hao, X. Wang, J. Mi, L. Jiang, Q. Yu, Microstructure and thermal stability of Al/$Ti_{0.5}Al_{0.5}N$/$Ti_{0.25}Al_{0.75}N$/AlN solar selective coating, Solar energy materials and solar cells, 111 (2013) 49-56.

[5] X. Paquez, G. Amiard, G. de Combarieu, C.d. Boissière, D. Grosso, Resistant RuO_2/SiO_2 absorbing sol–gel coatings for solar energy conversion at high temperature, Chemistry of Materials, 27 (2015) 2711-2717.

[6] N. Selvakumar, N.T. Manikandanath, A. Biswas, H.C. Barshilia, Design and fabrication of highly thermally stable HfMoN/HfON/Al_2O_3 tandem absorber for solar thermal power generation applications, Solar Energy Materials and Solar Cells, 102 (2012) 86-92.

[7] X.-H. Gao, W. Theiss, Y.-Q. Shen, P.-J. Ma, G. Liu, Optical simulation, corrosion behavior and long term thermal stability of TiC-based spectrally selective solar absorbers, Solar Energy Materials and Solar Cells, 167 (2017) 150-156.

[8] A. Amri, Z.-T. Jiang, T. Pryor, C.-Y. Yin, Z. Xie, N. Mondinos, Optical and mechanical characterization of novel cobalt-based metal oxide thin films synthesized using sol–gel dip-coating method, Surface and Coatings Technology, 207 (2012) 367-374.
[9] S. Sklarew, Emittance studies of various high temperature materials and coatings, in, MARQUARDT CO VAN NUYS CA, 1963.
[10] A. Soum-Glaude, A. Le Gal, M. Bichotte, C. Escape, L. Dubost, Optical characterization of $TiAlN_x/TiAlN_y/Al_2O_3$ tandem solar selective absorber coatings, Solar Energy Materials and Solar Cells, 170 (2017) 254-262.
[11] I. Setién-Fernández, T. Echániz, L. González-Fernández, R.B. Pérez-Sáez, E. Céspedes, J.A. Sánchez-García, L. Álvarez-Fraga, R.E. Galindo, J.M. Albella, C. Prieto, First spectral emissivity study of a solar selective coating in the 150–600° C temperature range, Solar Energy Materials and Solar Cells, 117 (2013) 390-395.
[12] T. Echániz, I. Setién-Fernández, R.B. Pérez-Sáez, C. Prieto, R.E. Galindo, M.J. Tello, Importance of the spectral emissivity measurements at working temperature to determine the efficiency of a solar selective coating, Solar Energy Materials and Solar Cells, 140 (2015) 249-252.
[13] J. Jyothi, A. Soum-Glaude, H.S. Nagaraja, H.C. Barshilia, Measurement of high temperature emissivity and photothermal conversion efficiency of TiAlC/TiAlCN/TiAlSiCN/TiAlSiCO/TiAlSiO spectrally selective coating, Solar Energy Materials and Solar Cells, 171 (2017) 123-130.
[14] A. Dan, J. Jyothi, K. Chattopadhyay, H.C. Barshilia, B. Basu, Spectrally selective absorber coating of $WAlN/WAlON/Al_2O_3$ for solar thermal applications, Solar Energy Materials and Solar Cells, 157 (2016) 716-726.
[15] A. Dan, K. Chattopadhyay, H.C. Barshilia, B. Basu, Thermal stability of $WAlN/WAlON/Al_2O_3$ - based solar selective absorber coating, MRS Advances, CJO2016. (2016) doi:10.1557/adv.2016.1388.

.
[16] A. Dan, K. Chattopadhyay, H.C. Barshilia, B. Basu, Angular solar absorptance and thermal stability of $W/WAlN/WAlON/Al_2O_3$-based solar selective absorber coating, Applied Thermal Engineering, 109 (2016) 997-1002.
[17] A. Dan, K. Chattopadhyay, H.C. Barshilia, B. Basu, Colored selective absorber coating with excellent durability, Thin Solid Films, 620 (2016) 17-22.
[18] V.K.W. Grips, H.C. Barshilia, V.E. Selvi, K.S. Rajam, Electrochemical behavior of single layer CrN, TiN, TiAlN coatings and nanolayered TiAlN/CrN multilayer coatings prepared by reactive direct current magnetron sputtering, Thin solid films, 514 (2006) 204-211.
[19] W.C. Oliver, G.M. Pharr, An improved technique for determining hardness and elastic modulus using load and displacement sensing indentation experiments, Journal of materials research, 7 (1992) 1564-1583.
[20] C.-D. Wen, I. Mudawar, Experimental investigation of emissivity of aluminum alloys and temperature determination using multispectral radiation thermometry (MRT) algorithms, Journal of materials engineering and performance, 11 (2002) 551-562.
[21] G. Corro, J.L.G. Fierro, V.C. Odilon, An XPS evidence of Pt^{4+} present on sulfated Pt/Al_2O_3 and its effect on propane combustion, Catalysis Communications, 4 (2003) 371-376.
[22] H. Lu, C.L. Bao, D.H. Shen, X.J. Zhang, Y.D. Cui, Z.D. Lin, Study of the Ti/Al_2O_3 interface, Journal of materials science, 30 (1995) 339-346.
[23] L. Salvati Jr, L.E. Makovsky, J.M. Stencel, F.R. Brown, D.M. Hercules, Surface spectroscopic study of tungsten-alumina catalysts using X-ray photoelectron, ion scattering, and Raman spectroscopies, The Journal of Physical Chemistry, 85 (1981) 3700-3707.
[24] L.J. Saethre, N. Martensson, S. Svensson, P.A. Malmquist, U. Gelius, K. Siegbahn, Gas phase ESCA studies of 2, 5-diaza-1, 6-dioxa-6a-thiapentalene and its selenium and tellurium analogs, Journal of the American Chemical Society, 102 (1980) 1783-1788.

[25] T.H. Fleisch, G.J. Mains, An XPS study of the UV reduction and photochromism of MoO_3 and WO_3, The Journal of Chemical Physics, 76 (1982) 780-786.
[26] K.A. O'Donnell, E.R. Mendez, Experimental study of scattering from characterized random surfaces, JOSA A, 4 (1987) 1194-1205.
[27] D.W. Berreman, Infrared absorption at longitudinal optic frequency in cubic crystal films, Physical Review, 130 (1963) 2193-2198.
[28] M. Kaltchev, W.T. Tysoe, An infrared spectroscopic investigation of thin alumina films: measurement of acid sites and surface reactivity, Surface science, 430 (1999) 29-36.
[29] C.-T. Hsieh, J.-M. Chen, R.-R. Kuo, T.-S. Lin, C.-F. Wu, Influence of surface roughness on water- and oil-repellent surfaces coated with nanoparticles, Applied Surface Science, 240 (2005) 318-326.
[30] S.K. Rawal, A.K. Chawla, V. Chawla, R. Jayaganthan, R. Chandra, Structural, optical and hydrophobic properties of sputter deposited zirconium oxynitride films, Materials Science and Engineering: B, 172 (2010) 259-266.
[31] M.M. Gentleman, J.A. Ruud, Role of hydroxyls in oxide wettability, Langmuir, 26 (2009) 1408-1411.
[32] A.A. Tsyganenko, P.P. Mardilovich, Structure of alumina surfaces, Journal of the Chemical Society, Faraday Transactions, 92 (1996) 4843-4852.
[33] K.M. Pertays, G.E. Thompson, M.R. Alexander, Self-assembly of stearic acid on aluminium: the importance of oxide surface chemistry, Surface and interface analysis, 36 (2004) 1361-1366.
[34] H. Alanyali, R.M. Souto, Research on the corrosion behavior of TiN-TiAlN multilayer coatings deposited by cathodic-arc ion plating, Corrosion, 59 (2003) 851-853.
[35] M. Mazur, M. Kalisz, J. Domaradzki, M. Grobelny, D. Wojcieszak, D. Kaczmarek, A. Poniedziałek, Comparison of structural, mechanical and corrosion properties of (Ti 0.68 W 0.32) O x and (Ti 0.41 W 0.59) O x thin films, deposited on TiAlV surface by electron beam evaporation, Surface and Coatings Technology, 307 (2016) 596-602.
[36] S.J. Yuan, S.O. Pehkonen, Y.P. Ting, E.T. Kang, K.G. Neoh, Corrosion behavior of type 304 stainless steel in a simulated seawater-based medium in the presence and absence of aerobic Pseudomonas NCIMB 2021 bacteria, Industrial & Engineering Chemistry Research, 47 (2008) 3008-3020.
[37] F.M. Gao, L.H. Gao, Microscopic models of hardness, Journal of superhard materials, 32 (2010) 148-166.
[38] H.C. Barshilia, B. Deepthi, A.S.A. Prabhu, K.S. Rajam, Superhard nanocomposite coatings of TiN/Si_3N_4 prepared by reactive direct current unbalanced magnetron sputtering, Surface and Coatings Technology, 201 (2006) 329-337.
[39] N. Vidakis, A. Antoniadis, N. Bilalis, The VDI 3198 indentation test evaluation of a reliable qualitative control for layered compounds, Journal of materials processing technology, 143 (2003) 481-485.
[40] T. Satō, Spectral emissivity of silicon, Japanese Journal of Applied Physics, 6 (1967) 339.
[41] E. Brodu, M. Balat-Pichelin, J.L. Sans, M.D. Freeman, J.C. Kasper, Efficiency and behavior of textured high emissivity metallic coatings at high temperature, Materials & Design, 83 (2015) 85-94.
[42] J. Labed, M.P. Stoll, Angular variation of land surface spectral emissivity in the thermal infrared: laboratory investigations on bare soils, Remote Sensing, 12 (1991) 2299-2310.
[43] A.E. Wald, J.W. Salisbury, Thermal infrared directional emissivity of powdered quartz, Journal of Geophysical Research: Solid Earth, 100 (1995) 24665-24675.
[44] A. Maturilli, J. Helbert, S. Ferrari, M. D'Amore, On the effect of emergence angle on emissivity spectra: application to small bodies, Earth, Planets and Space, 68 (2016) 84.
[45] V. García-Santos, E. Valor, V. Caselles, M. Ángeles Burgos, C. Coll, On the angular variation of thermal infrared emissivity of inorganic soils, Journal of Geophysical Research: Atmospheres, 117 (2012).

[46] O. Rozenbaum, D.D.S. Meneses, Y. Auger, S. Chermanne, P. Echegut, A spectroscopic method to measure the spectral emissivity of semi-transparent materials up to high temperature, Review of scientific instruments, 70 (1999) 4020-4025.
[47] C.W. Lee, Y.T. Kim, High temperature thermal stability of plasma-deposited tungsten nitride Schottky contacts to GaAs, Solid-state electronics, 38 (1995) 679-682.
[48] L. Hultman, Thermal stability of nitride thin films, Vacuum, 57 (2000) 1-30.
[49] L. Rebouta, A. Pitães, M. Andritschky, P. Capela, M.F. Cerqueira, A. Matilainen, K. Pischow, Optical characterization of TiAlN/TiAlON/SiO_2 absorber for solar selective applications, Surface and Coatings Technology, 211 (2012) 41-44.
[50] L. Gaouyat, F. Mirabella, O. Deparis, Critical tuning of magnetron sputtering process parameters for optimized solar selective absorption of $NiCrO_x$ cermet coatings on aluminium substrate, Applied surface science, 271 (2013) 113-117.
[51] H.C. Barshilia, N. Selvakumar, K.S. Rajam, A. Biswas, Spectrally selective NbAlN/NbAlON/Si_3N_4 tandem absorber for high-temperature solar applications, Solar energy materials and solar cells, 92 (2008) 495-504.
[52] C. Zou, W. Xie, L. Shao, Functional multi-layer solar spectral selective absorbing coatings of AlCrSiN/AlCrSiON/AlCrO for high temperature applications, Solar Energy Materials and Solar Cells, 153 (2016) 9-17.
[53] Y. Wu, C. Wang, Y. Sun, Y. Ning, Y. Liu, Y. Xue, W. Wang, S. Zhao, E. Tomasella, A. Bousquet, Study on the thermal stability of Al/NbTiSiN/NbTiSiON/SiO_2 solar selective absorbing coating, Solar Energy, 119 (2015) 18-28.

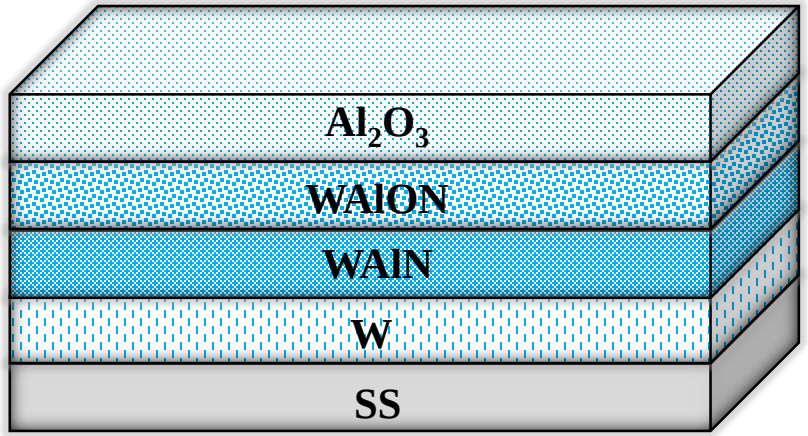

Fig. 1. Schematic representation of W/WAlN/WAlON/Al_2O_3 –based absorber coating on SS substrate deposited by magnetron sputtering.

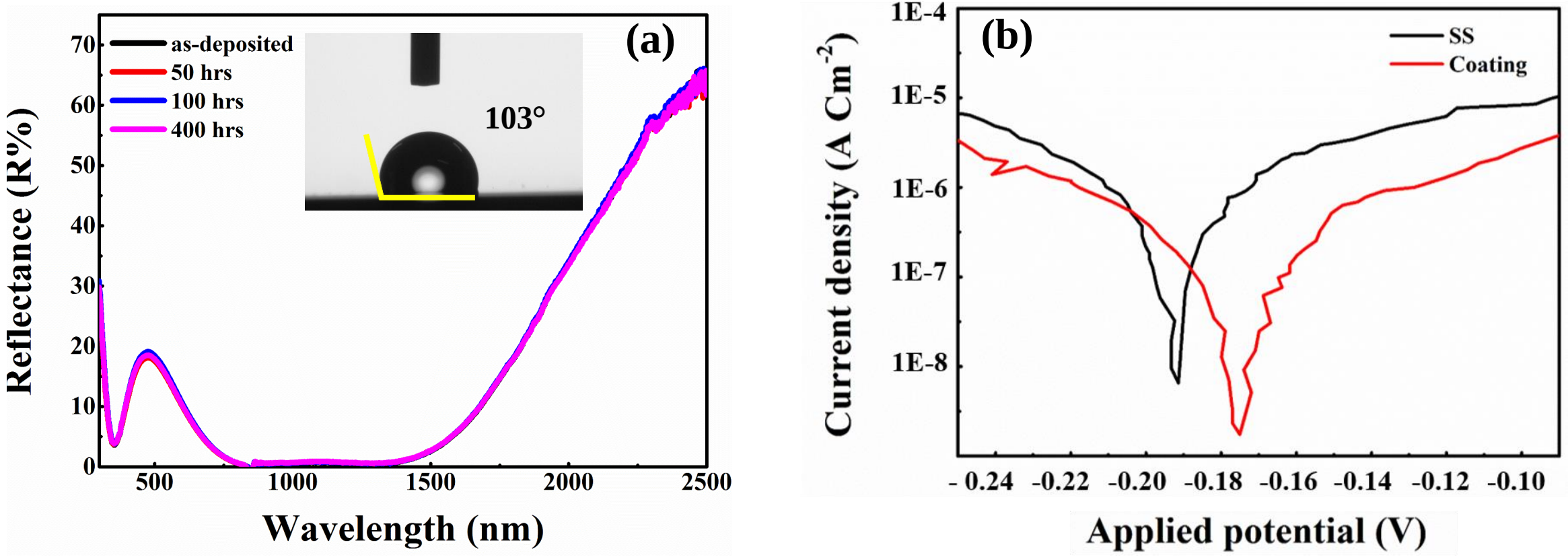

Fig. 2. (a) Reflectance spectra of the coating before and after humidity test at 37 °C and 95% condensation. The inset shows the contact angle at water-coating interface, (b) Potentiodynamic polarization curves of uncoated SS and W/WAlN/WAlON/Al_2O_3 coating, in 3.5% NaCl solution.

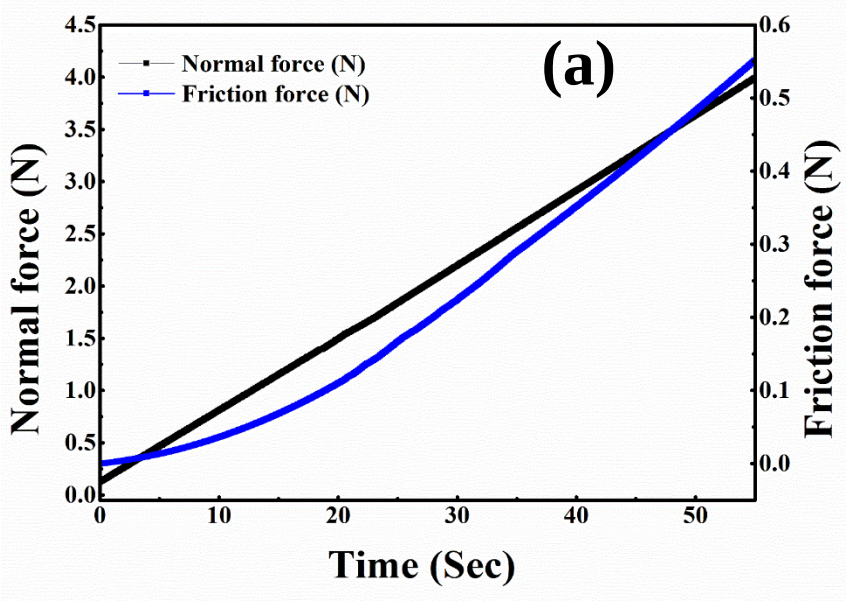

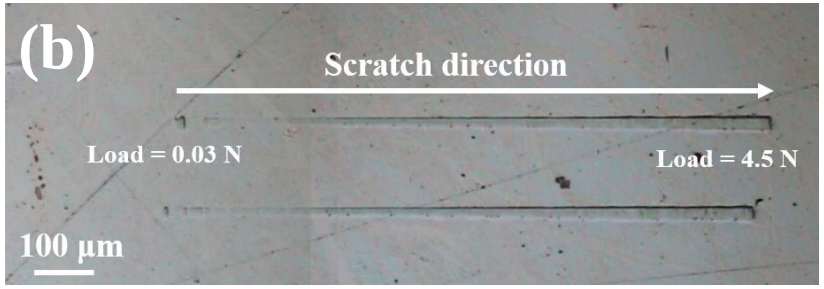

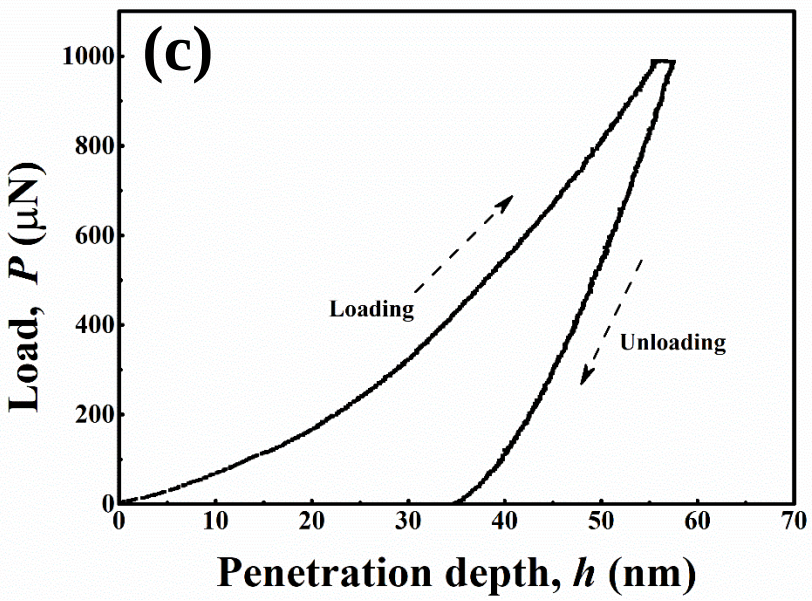

Fig. 3. (a) Evaluation of adhesion properties by performing nano - scratch test, showing graphs of normal load (N) and friction force (N) vs. time (s), (b) Optical micrograph of the scratch track at a linearly increasing normal load from 1 to 4.5 N, (c) Load-Penetration depth response of W/WAlN/WAlON/Al_2O_3 thin film.

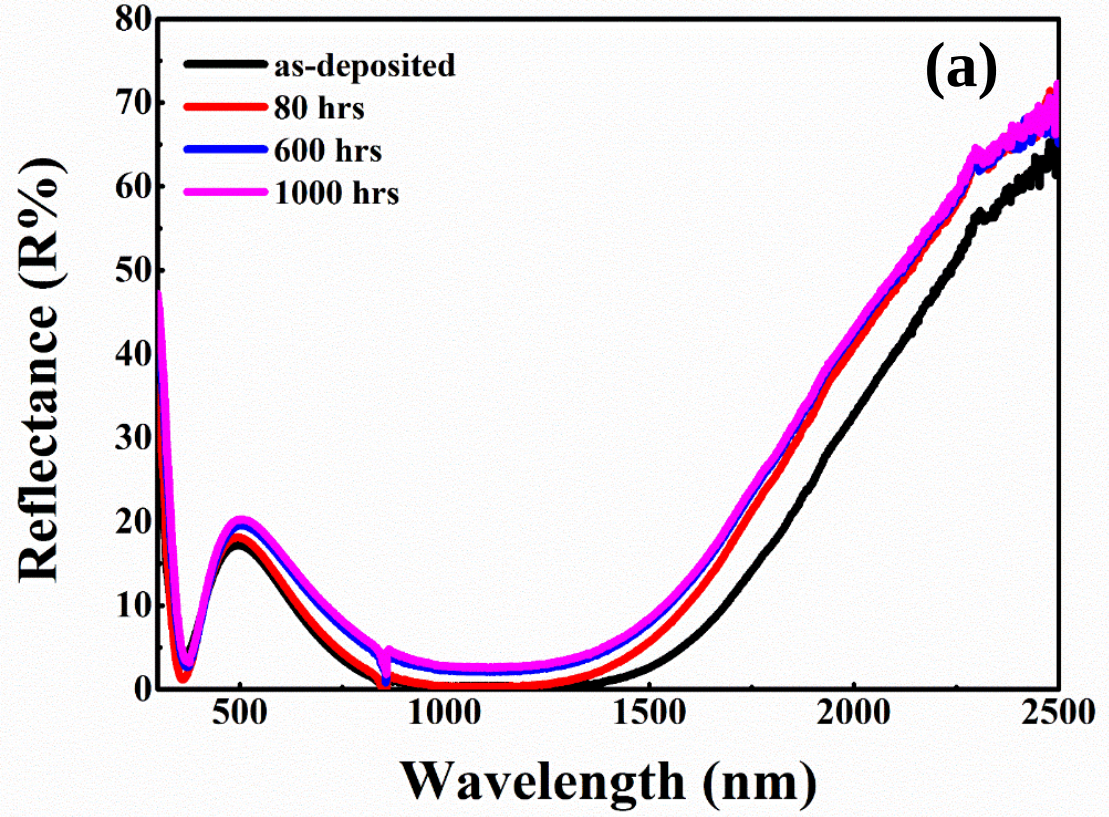

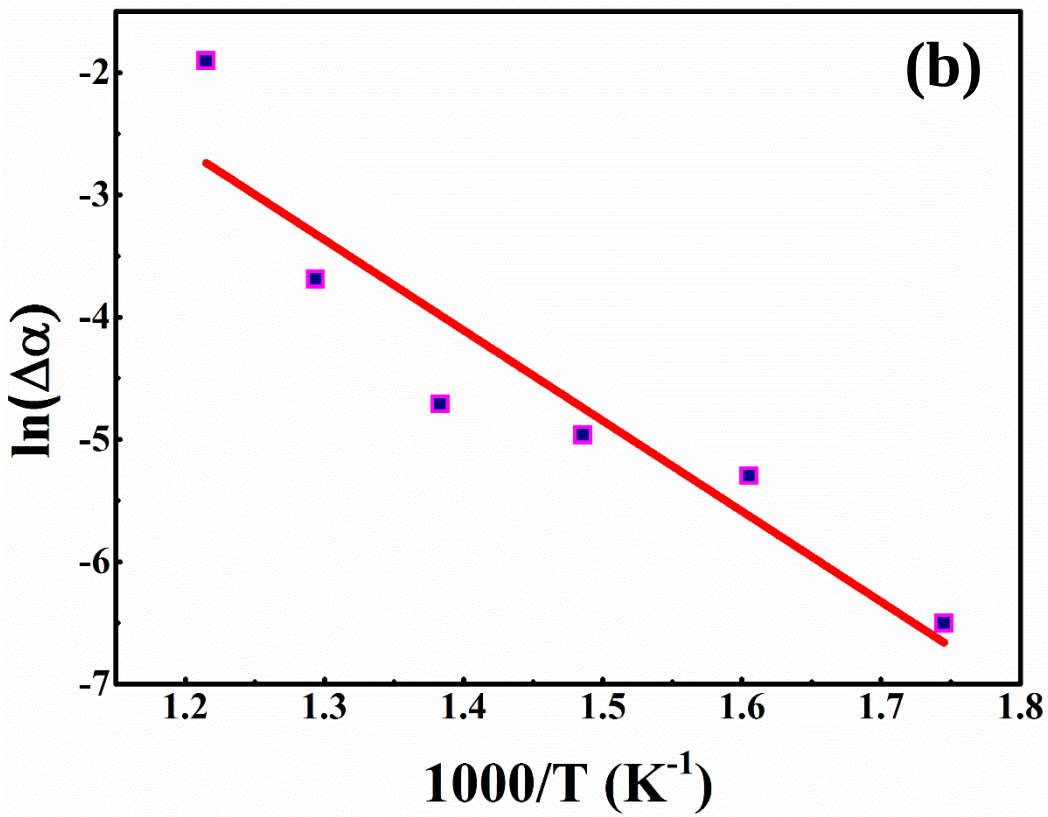

Fig. 4. (a) Reflectance spectra of the coating after heat treatment at 350 °C for 1000 hrs in air. (b) Arrhenius plot for the degradation of the coating heat treated at 300, 400, 500 and 550 °C for 2 hrs in air. Solid line indicates linear fit.

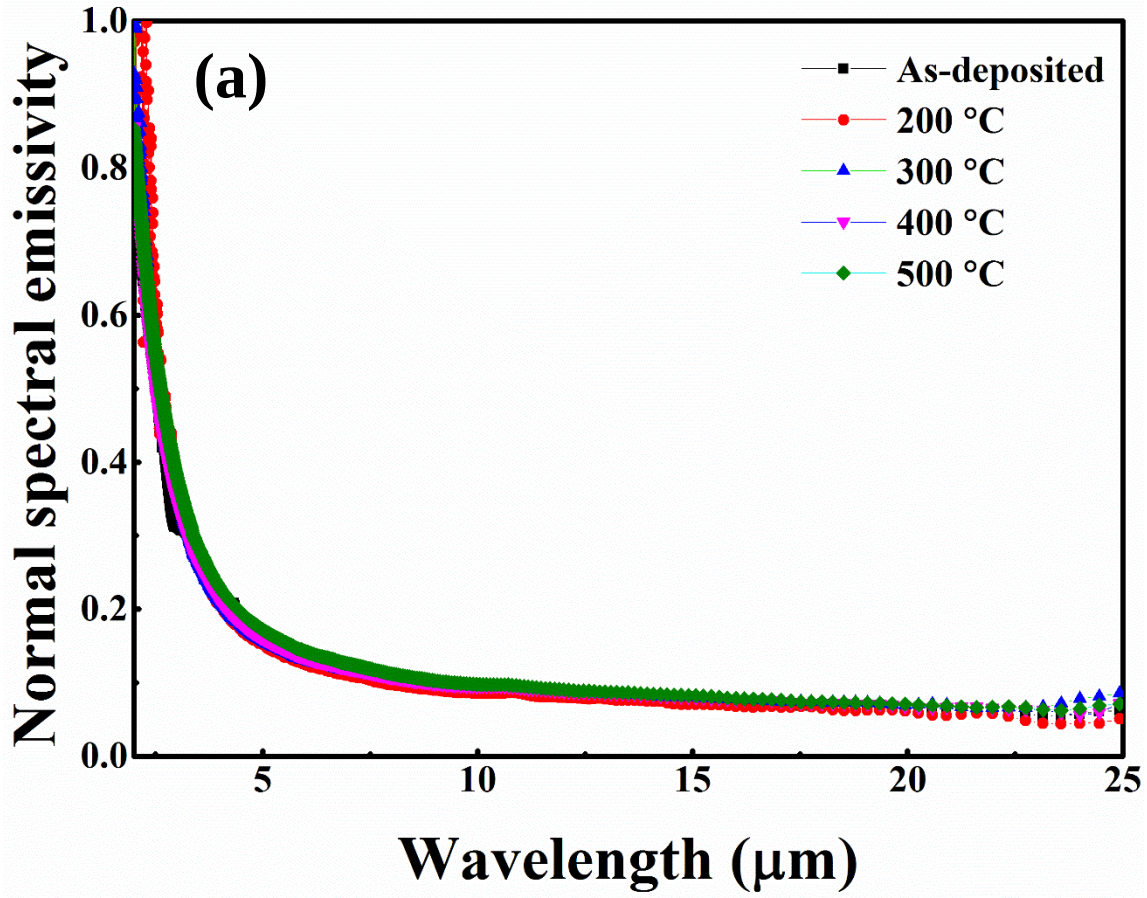

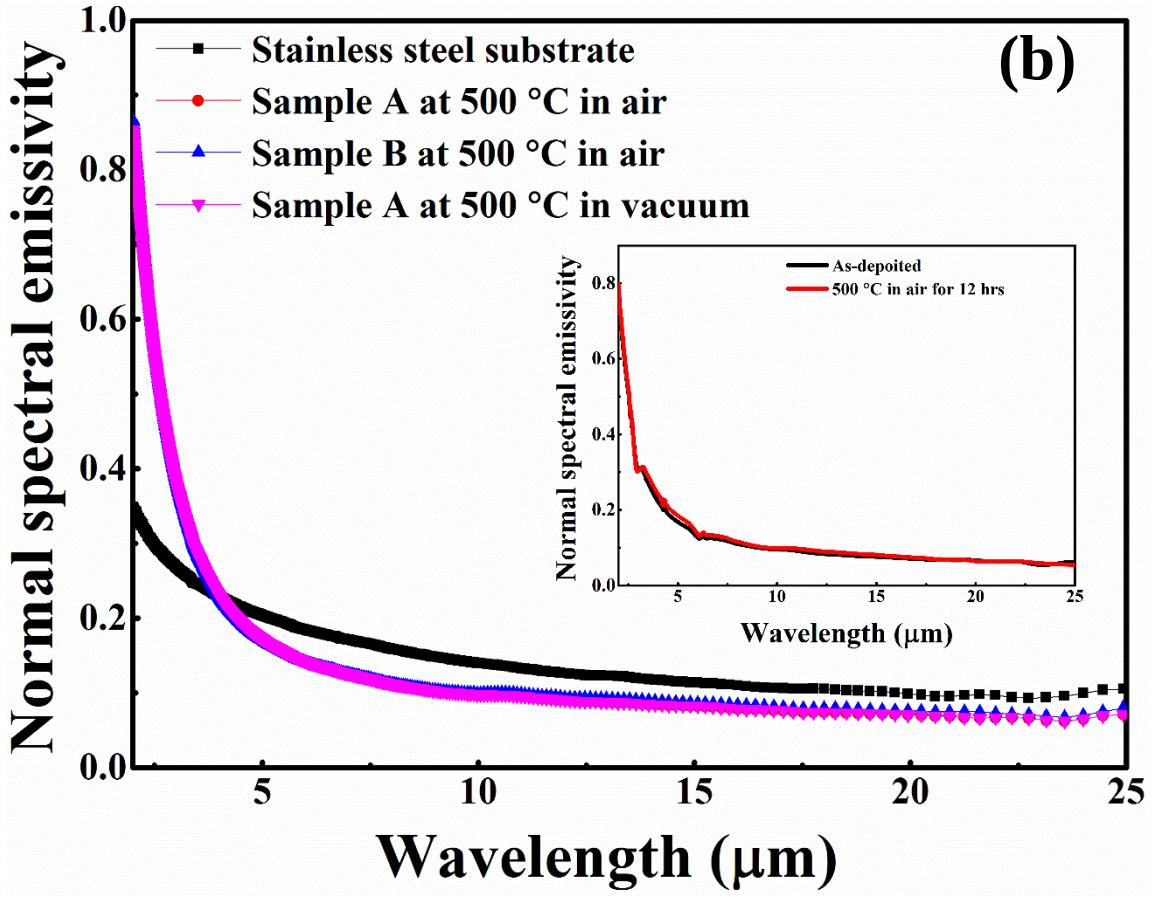

Fig. 5. (a) Temperature dependence of the normal spectral emissivity at different temperatures. (b) Comparison between the spectral emissivity of SS substrate and that of W/WAlN/WAlON/Al_2O_3 coating (sample A and sample B, both having identical compositional architechture) at highest measured temperature of 500 °C. Evaluation of normal spectral emissivity of the coating after annealing at 500 °C in air for 12 hrs.

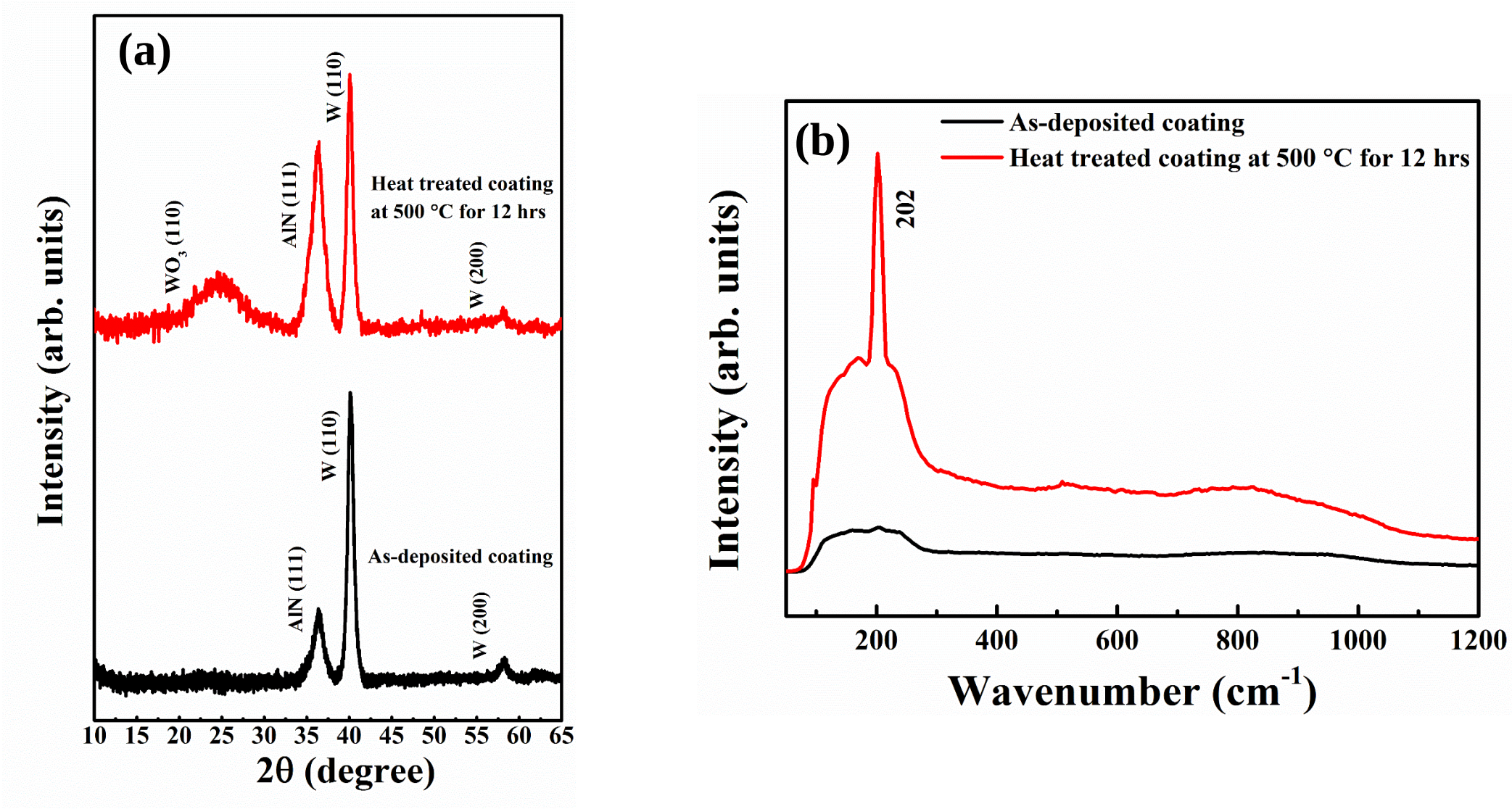

Fig. 6. (a) XRD and (b) Raman spectrum analysis of as-deposited and annealed coating at 500 °C for 12 hrs in air. The presence of WO_3 is evident in the annealed coating.

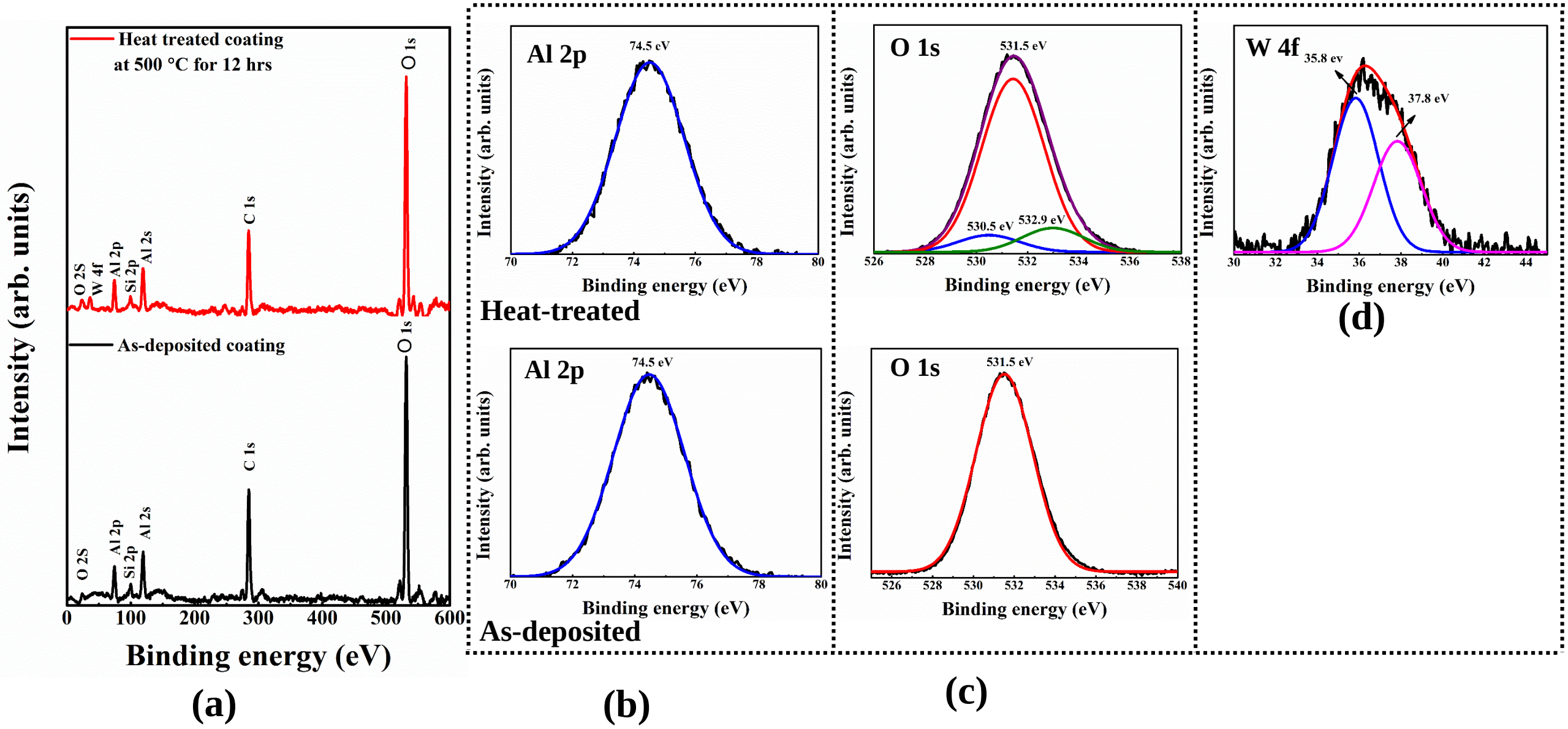

Fig. 7. (a) XPS survey spectra, (b) Al 2p, (c) O 1s core level spectra of as-deposited and annealed coating at 500 °C in air for 12 hr, (d) core level W 4f spectra of heat-treated coating.

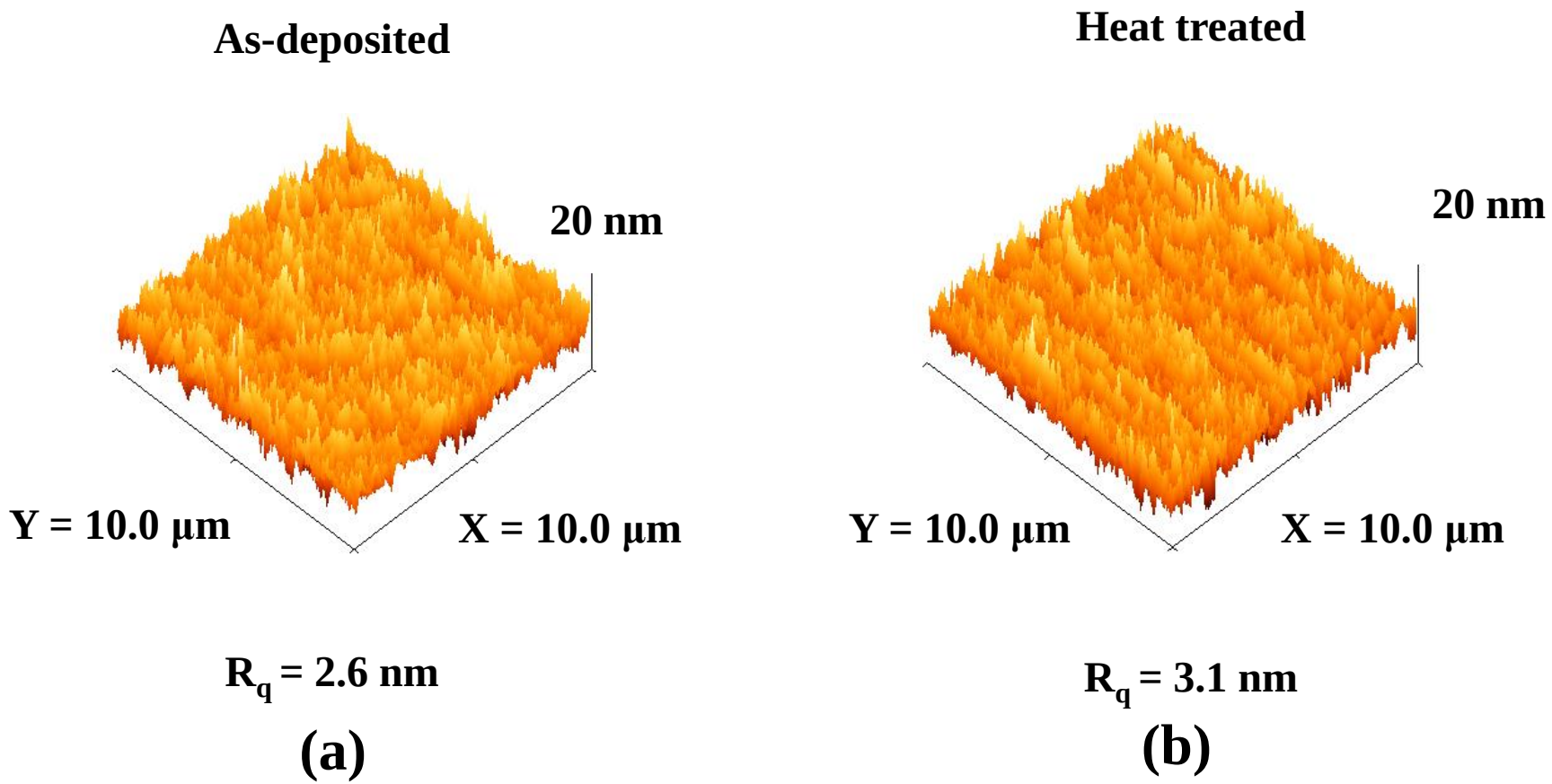

Fig. 8. 3D AFM images of (a) as-deposited and (b) annealed coating in air at 500 °C for 12 hrs in air.

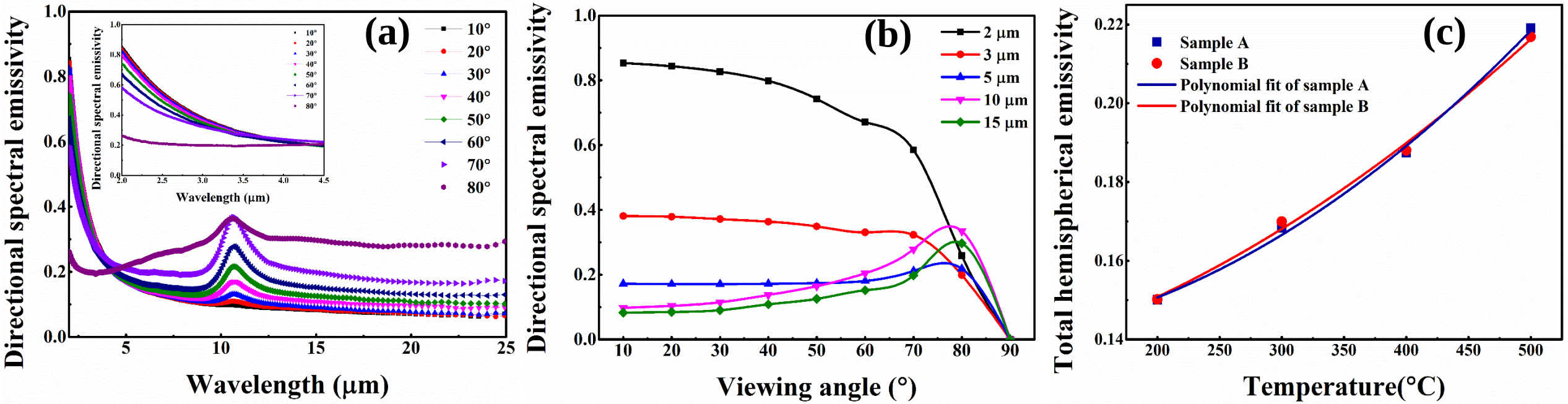

Fig. 9. (a) Directional emissivity of the coating as a (a) function of wavelength for entire wavelength range. (b) function of viewing angle for five wavelengths as at 500 °C. The points have been joined with cubic splines for better visualization of the tendencies. (c) Temperature dependence of total hemispherical emissivity of sample A and sample B, fitted to polynomials of order 2

Table 1. The absorptance and emittance values of W/WAlN/WAlON/Al_2O_3 coating before and after annealing for 2 hrs in air

Temperature (°C)	Absorptance (α)			Emittance (ε)		
	As-deposited	Annealed	$\Delta\alpha$	As-deposited	Annealed	$\Delta\varepsilon$
300	0.959	0.957	0.002	0.08	0.08	0.00
350	0.959	0.954	0.005	0.08	0.08	0.00
400	0.959	0.952	0.007	0.08	0.08	0.00
450	0.959	0.950	0.009	0.08	0.08	0.00
500	0.959	0.934	0.025	0.08	0.11	0.03
550	0.959	0.810	0.149	0.08	0.50	0.42